Identification of Rigosertib for the Treatment of Recessive Dystrophic Epidermolysis Bullosa–Associated Squamous Cell Carcinoma

Atanasova, Velina S.; Pourreyron, Celine; Farshchian, Mehdi; Lawler, Michael E.; Brown, Christian A.; Watt, Stephen

Published in:
Clinical Cancer Research

DOI:
10.1158/1078-0432.CCR-18-2661

Publication date:
2019

Document Version
Peer reviewed version

Identification of rigosertib for the treatment of recessive dystrophic epidermolysis bullosa-associated squamous cell carcinoma

Velina S. Atanasova[1♦], Celine Pourreyron[2♦], Mehdi Farshchian[1], Michael Lawler[1], Christian A. Brown IV[1], Stephen A. Watt[2], Sheila Wright[2], Michael Warkala[1], Christina Guttmann-Gruber[3], Josefina Piñón Hofbauer[3], Ignacia Fuentes[4,5], Marco Prisco[1], Elham Rashidghamat[6], Cristina Has[7], Julio C. Salas-Alanis[8], Francis Palisson[4,9], Alain Hovnanian[10,11], John A. McGrath[6], Jemima E. Mellerio[6], Johann W. Bauer[3], Andrew P. South[1*].

[1]Department of Dermatology and Cutaneous Biology, Thomas Jefferson University, Philadelphia, PA

[2]Division of Cellular Medicine, University of Dundee, Dundee, UK

[3]EB House Austria, Research Program for Molecular Therapy of Genodermatoses, Department of Dermatology, University Hospital Salzburg, Paracelsus Medical University Salzburg, Austria

[4]Fundación DEBRA Chile, Santiago, Chile

[5]Centro de Genética y Genómica, Facultad de Medicina Clínica Alemana, Universidad del Desarrollo, Santiago, Chile

[6]St. John's Institute of Dermatology, King's College London (Guy's Campus), London, UK

[7]Department of Dermatology, Medical Center – University of Freiburg, Faculty of Medicine, Freiburg, Germany

[8]Instituto Dearmatologico de Jalisco, Guadalajara, Mexico.

[9]Facultad de Medicina Clínica Alemana, Universidad del Desarrollo, Santiago, Chile

[10]INSERM UMR 1163, Paris, France;

[11]Imagine Institute, Paris, France

Running title: Rigosertib for RDEB SCC therapy

Keywords (5): squamous cell carcinoma, recessive dystrophic epidermolysis bullosa, PLK1, Microtubule, RAS, CRAF, MEK, AKT

Financial support: This work was supported by DEBRA International – funded by DEBRA UK (grant to APS, and grant to APS, JWB, and JEM) and the Office of the Assistant Secretary of Defense for Health Affairs and the Defense Health Agency J9, Research and Development Directorate, through the Congressionally Directed Medical Research Program under Award No. (W81XWH-18-1-0382 to APS). Opinions, interpretations, conclusions and recommendations are those of the authors and are not necessarily endorsed by the Department of Defense. M.F. is supported by the Sigrid Juse´lius Foundation, Orion Research Foundation, and the Finnish Society of Dermatology.

* *Correspondence:* Dr. Andrew P South, Dermatology and Cutaneous Biology, Thomas Jefferson University, 233 S. 10th Street, BLSB 406, Philadelphia, PA. Tel: (215) 955 1934; Fax: (215) 503 5774. E-mail: Andrew.south@Jefferson.edu.

[φ] These authors contributed equally to this work.

The authors state no conflict of interests.

Word count: 3,059

Number of figures and tables: 6

Statement of translational relevance

Collectively our data support a clinical trial of rigosertib for treatment of recessive dystrophic epidermolysis bullosa-associated squamous cell carcinoma, an inherently aggressive sub-type of squamous cell carcinoma with extremely low 5-year survival. Currently there are no effective treatments for this devastating cancer and often times initial SCC will recur and readily metastasize; any effective systemic therapy that reduces tumor burden will improve quality of life in this patient population.

Abstract

Purpose: Squamous cell carcinoma (SCC) of the skin is the leading cause of death in patients with the severe generalized form of the genetic disease recessive dystrophic epidermolysis bullosa (RDEB). Although emerging data are identifying why patients suffer this fatal complication, therapies for treatment of RDEB SCC are in urgent need.

Experimental Design: We previously identified polo-like kinase 1 (PLK1) as a therapeutic target in skin SCC, including RDEB SCC. Here, we undertake a screen of 6 compounds originally designated as PLK1 inhibitors, and detail the efficacy of the lead compound, the multi-pathway allosteric inhibitor ON-01910, for targeting RDEB SCC in vitro and in vivo.

Results: ON-01910 (or rigosertib) exhibited significant specificity for RDEB SCC: in culture rigosertib induced apoptosis in 10/10 RDEB SCC keratinocyte populations while only slowing the growth of normal primary skin cells at doses 2 orders of magnitude higher. Furthermore, rigosertib significantly inhibited the growth of two RDEB SCC in murine xenograft studies with no apparent toxicity. Mechanistically rigosertib has been shown to inhibit multiple signaling pathways. Comparison of PLK1 siRNA with MEK inhibition, AKT inhibition, and the microtubule disrupting agent vinblastine in RDEB SCC shows that only PLK1 reduction exhibits a similar sensitivity profile to rigosertib.

Conclusions: These data support a "first in RDEB" phase II clinical trial of rigosertib to assess tumor targeting in patients with late stage, metastatic and/ or unresectable SCC.

Introduction

Patients with the devastating inherited skin disease recessive dystrophic epidermolysis bullosa (RDEB) are at significantly increased risk of developing aggressive cutaneous squamous cell carcinoma (SCC), which is the cause of death by age 45 years in 70% of individuals with the severe generalized form of the disease(1, 2). Furthermore, 5 year survival in all RDEB sub-types diagnosed with SCC is close to 0% (2) making RDEB SCC one of the most aggressive forms of this tumor type. Current clinical guidelines offer limited treatment options for RDEB SCC and consist of wide local excision, radiotherapy, and in late stages, limb amputation (3). New approaches to therapy for RDEB SCC are in urgent need.

RDEB is caused by mutations in *COL7A1*, the gene encoding type VII collagen (4). However, *COL7A1* does not behave as a classical tumor suppressor as heterozygous carriers are not at increased risk of skin cancer and *COL7A1* has not been identified as a significantly mutated gene in genetic profiling of any tumor type to date. RDEB is characterized by skin fragility, trauma induced skin blistering, and chronic non-healing wounds (5) and work by us and others has implicated the tumor microenvironment as a driving mechanism of cancer development (6, 7). Our recent comprehensive genetic characterization of RDEB SCC demonstrates that these tumors are driven by somatic mutation in driver genes that are identical to UV-induced skin SCC and head and neck SCC (HNSCC) (8) and we have consistently been unable to identify genetic mechanisms which explain the aggressive nature of RDEB SCC (9, 10). Our early microarray gene expression profiling failed to significantly differentiate RDEB from skin SCC in cultured keratinocytes (10). However, this work did identify polo-like kinase 1 (PLK1) as a therapeutic target in RDEB SCC.

Here we follow up this finding with a screen of compounds originally designated as PLK1 inhibitors and identify ON-01910, or rigosertib, as a lead candidate for therapy in RDEB SCC.

Materials and Methods

Cell cultures

Cells were isolated from biopsies taken as part of routine surgical or diagnostic procedures. Informed written consent was obtained from each patient or in the case of under-aged children from their parents or guardian. Ethical approval for this investigation was obtained from all local ethics committees, and this study was performed in accordance with the Helsinki declaration. All cells were isolated as described (11) and cultured at 37° C in 5% CO_2. Keratinocytes were grown in Dulbecco's modified essential medium (DMEM, Corning cellgro, Mediatech Inc, Manassas, VA)/ Ham's F12 medium (3:1), supplemented with 10% fetal bovine serum (FBS, PEAK Serum, Cat PS-FB1, Colorado, USA), 10 ng/ml of epidermal growth factor, 10^{-10} M cholera toxin, 0.4 µg/ml of hydrocortisone, 5 µg/ml of transferrin, 5 µg/ml of insulin and 13 ng/ml liothyronine. Supplementary data ***Table S1*** details all cells used in this study. All cells are routinely tested for *Mycoplasma* using either a PCR approach or a colorimetric detection assay (MycoAlert™, Lonza, Allendale, NJ). SCCRDEB2, SCCRDEB3, SCCRDEB70, RDEB84 and RDEB86 were *Mycoplasma* positive upon isolation and were treated with Plasmocure™ (InvivoGen, San Diego, CA). Only cells which yielded a negative *Mycoplasma* test were used in the assays described.

Protein Quantification

Total lysates were quantified using Pierce bicinchoninic assay Protein Assay kit (Fisher Scientific, Waltham, MA, cat# 23225) and 5-50 µg of protein were loaded onto SDS-PAGE gel. The signal

from Western blot analysis was quantified with Image J. P-CRAF and P-AKT were quantified relative to GAPDH.

Drug treatment and western blot analysis

Rigosertib (ON 01910.Na) was either purchased from Selleckchem.com (Houston, TX) or provided by Onconova Therapeutics, Inc. (Newtown, PA). All other drugs were purchased from Selleckchem.com. 2-4 x 10^5 keratinocytes were plated in a 6 well dish. On the following day, the medium was changed with the drug at 1 µM or vehicle control. Medium was left for 48 hours and cells were lysed with radioimmunoprecipitation assay buffer. Lysate was placed in a centrifuge for 5 minutes at 4^{o}C, and the supernatant was mixed with a 6x Laemmli loading buffer. Samples were boiled for 5 minutes at 95^{o}C before being loaded onto SDS-PAGE gels. Primary antibodies used were: PLK1 (Cell Signaling, 208G4), CRAF polyclonal (Cell signaling, 9422S), P-CRAF (Cell signaling, 9427S), P-AKT (Cell signaling, 9271), AKT (Cell signaling, 9272), GAPDH (Santa Cruz Biotechnology, 6C5). Resolved proteins were transferred onto nitrocellulose membrane with a BioRad Trans-Blot-Turbo (Bio-Rad, Hercules, CA), blocked in TBS-0.1% Tween with 5% milk or 5% BSA according to requirements of the primary antibody, and incubated overnight with the primary antibody. After incubation with IgG-HRP conjugated secondary antibody (Santa Cruz Biotechnology), membrane was incubated with Pierce ECL Western blotting substrate (Fisher Scientific) and exposed to CL-XPosure X-ray film (Fisher Scientific).

Immunofluorescence

RDEB SCC and human control skin biopsies were frozen in optimal cutting temperature (OCT, Sakura Finetek USA, Torrance, CA) and cut at 6 microns on a cryostat. Sections were fixed with 50:50 methanol: acetone mixture for 5 minutes. Slides were rinsed with 1x PBS, permeabilized with PBS/0.1% Tween 20 (Sigma Aldrich, St. Louis, MO) for 5 minutes followed by blocking for 1 hour with PBST/3% BSA (Sigma Aldrich). Primary antibodies were incubated for 1.5 hours at room temperature. Secondary antibody Alexa Fluor 594 goat anti-rabbit (1:800, Molecular Probes Eugene, OR) was applied for 1 hour at room temperature. Slides were cover-slipped with hard set 4,6-diamidino-2-phenylindole (DAPI; Vector Labs, Burlingame, CA) and examined by fluorescence microscopy (EVOS FL cell imaging system, ThermoFisher).

Cell growth and metabolism assays

Colorimetric assays of mitochondrial dehydrogenase activity were performed using the MTS CellTitre 96 AQueous One Solution Cell Proliferation Assay (Promega, Madison, WI, USA) according to the manufacturer's instructions. In each case 1-4 x 10^4 cells were seeded into replica 96-well plates and readings were taken at intervals up to a maximum of 96 h. We have previously shown that an increase in mitochondrial dehydrogenase activity using this assay directly correlates with primary non-SCC and SCC cell number determined using a CASY Model TT cell counter (Roche Diagnostics Ltd, West Sussex, UK) (10).

For Crystal violet assay of cell growth, 1-4 x 10^4 cells were seeded into replica 96-well plates and fixed with 70% ETOH at intervals up to a maximum of 96 h. After fixation wells were incubated with a solution of 0.2% crystal violet in 2% ETOH for 1 hour at room temperature followed by three washes with tap water. Plates were allowed to air dry and were then photographed and

100 μl of 70% ethanol was added to each well for 20 minutes, the plate was agitated to homogenize the solution and the absorbance at 595 nm was measured using a plate reader (Flexstation 3, Molecular Devices). For photographic quantification black and white images were produced using the threshold function in Adobe Photoshop C6 (Adobe) and quantified using the measure tool.

Cell Cycle analysis

5-Bromodeoxyuridine (BrdU; Sigma-Aldrich) was added to cells at 30 mM final concentration for 2 hours. Cells were collected and washed in phosphate-buffered saline, then fixed overnight in cold 70% ethanol. RNase A (Sigma) was added at 100 μg/ml, in 5% Tween-20 and phosphate-buffered saline for 30 minutes at 37°C. Pepsin (Sigma) was added at 1 mg/ml in 30mM HCL for 30 min at 37°C and DNA was denatured with 2N HCl containing 0.5% Tween-20 in phosphate-buffered saline for 30 min at 37°C. An anti-BrdU antibody (Invitrogen) diluted in phosphate-buffered saline/0.1% Tween/ 1% bovine serum albumin was added for 2 h followed by a wash with 1% BSA. After passing the cells through a 70 μm filter, Propidium iodide (Sigma) was added in the final wash step at a concentration of 25 mg/ml. Samples were analyzed using a FACScan flow cytometer and CellQuest software (Becton Dickinson).

Apoptosis ELISA

Apoptosis was measured using the Cell Death Detection ELISA^{PLUS} (ROCHE, cat# 11774425001). Briefly, non-SCC keratinocytes were plated at $5x10^3$ cells /well and SCC keratinocytes at $2.5x10^4$ cells /well in 96 well plates. On the next day the cells were treated with the drug (1uM) for 16 to

24 hours. Cells were lysed for 30 minutes and 20 µl of the lysate was incubated with 80 µl immunoreagent (Flexstation 3, Molecular Devices). After incubation the reaction was stopped with ABTS solution and absorbance was read using a plate reader at 405 nm and 490 nm.

siRNA knockdown

siRNA oligonucleotides targeting PLK1 (FlexiTube siRNA, Qiagen, Cat. #: 1027416), a negative scrambled control (AllStars Negative Control siRNA, Qiagen, Cat. #: SI03650318) and a positive cell death control (AllStars Hs Cell Death siRNA, Qiagen, Cat. #: SI04381048) were used. Cells were seeded in six-well plates at $2.5x10^5$ cells/well and 24 h later transfected with siRNA (40 nM final concentration) using Lipofectamine 2000 (Invitrogen, Carlsbad, CA, USA) diluted in Opti-MEM (Invitrogen) according to the manufacturer's instructions. Cells were left for 16-24h before being lysed for Western blotting or trypsinized and seeded in 96-well plates at $5x10^3$ cells/well in 100 µl of media. For comparison of siRNA with vinblastine cells were seeded directly in 96-well plates at $1x10^4$ cells/well in 100 µl of media and transfected 24 h later as described.

In vivo tumor growth and treatment

All animal experiments were conducted in accordance with UK Home Office (Project License # 60/4054) and Thomas Jefferson IACUC (Protocol # 01719) regulations. For tumorigenicity assays a suspension of 1–4 x 10^6 tumor cells was mixed with high-concentration Matrigel (Becton Dickinson, Oxford, UK) and injected subcutaneously into the flanks of adult female SCID Balb/c mice (between 6 and 12 weeks of age and 18-27g in weight) purchased from The Jackson Laboratories (stock # 001803) or from Taconic (Model # CB17SC). Tumors were measured by a

caliper and treatment began when volume reached 100-200mm^3. Animals were treated with 20mg/kg rigosertib dissolved in PBS and animals were distributed into treatment or vehicle control groups by alternating between treatment (1st animal to reach minimum 100mm^3) and vehicle control (2nd animal). For the experiment shown in Figure S1, 25 mice were injected with 4x10^6 SCCRDEB16 cells and BI-2536 treatment was included as a positive control for 2 animals where every third animal was allocated to this group. For the experiment shown in Figure 4, 20 mice were injected with 1x10^6 SCCRDEB106 cells. In all cases animals where tumors were attached to the rib-cage or growing superficially were sacrificed and not included in the experiment.

TUNEL analysis

Terminal deoxynucleotidyl transferase dUTP nick end labeling (TUNEL) was performed using the TACS2 TdT_Fluor In Situ Apoptosis Detection kit (Trevigen, Gaithersburg, MD) according to the manufacturer's instructions. Slides were fixed with mounting medium containing DAPI and were viewed under a fluorescence microscope using a 495nm filter.

Statistics

Paired two-tailed t-test was used for statistical analysis using Prism 8 (GraphPad Software, La Jolla, CA). EC_{50} values were calculated with nonlinear regression using Prism 8.

Results

PLK1 is increased in RDEB SCC

We previously identified PLK1 mRNA was increased in 4 RDEB SCC keratinocyte cultures compared with normal primary keratinocyte controls (10). Here we extend this observation to a total of 10 separate SCC populations and identify PLK1 increased in 10 of 10 fresh frozen RDEB SCC tissue samples using immuno-histochemistry (***Figure 1***).

ON-01910 emerges with the largest delta comparing growth in RDEB SCC and primary skin cells

After confirmation of increased PLK1 in all RDEB SCC assessed we set out to compare the efficacy of commercially available PLK1 inhibitors for targeting RDEB SCC. We initially assessed the effects of 6 PLK1 inhibitors on cell metabolism using an MTS assay after 48 hours exposure to normal primary keratinocytes (n=1), RDEB primary fibroblasts (n=4), and RDEB SCC keratinocytes (n=4) (***Table S2***). These data identified the compound ON-01910, also known as rigosertib, as having the greatest specificity for RDEB SCC keratinocytes when compared with normal primary keratinocytes and RDEB primary fibroblasts (***Table S2***).

Next, these data were confirmed in all 10 separate patient derived RDEB SCC cell lines using crystal violet uptake by live cells after 48-72 hours exposure to varying drug concentrations (***Figure 2A, B*** *and* ***Figure S1***). These data identified clear specificity for RDEB SCC keratinocytes when compared with primary normal or primary non-SCC RDEB keratinocytes. We also observed that whereas higher concentrations of rigosertib could inhibit the growth of non-SCC primary keratinocytes in culture (both RDEB and non-RDEB, ***Figure 2A*** and ***B***) no obvious signs of cell

death were evident while in RDEB SCC keratinocyte populations cell death was widespread (***Figure 2C***).

ON-01910 induces apoptosis in RDEB SCC keratinocytes

In agreement with our previous data using PLK1 siRNA and the PLK1 inhibitors BI-2536 and GW-843682 (10), as well as published studies of rigosertib (12-14), exposure of RDEB SCC keratinocytes to rigosertib induced cell cycle arrest and apoptosis (***Figure 3A-B***).

PLK1 siRNA knockdown mimics ON-01910 specificity in RDEB SCC keratinocytes

Since its identification as an inhibitor of PLK1, rigosertib has been shown to inhibit a variety of kinases, including AKT (12) and recently rigosertib has been shown to compete with activated RAS for binding to CRAF (15). More recently rigosertib was shown to bind to and destabilize microtubules (16) and studies in other malignancies have shown synthetic lethality of PLK1 and microtubule destabilizing agents (17).

To investigate potential mechanisms of action of rigosertib we first exposed RDEB SCC keratinocytes to inhibitors of MEK and AKT as well as the microtubule destabilizing agent vinblastine. These data showed some efficacy of MEK inhibition at lower concentrations but no specificity over normal cells at higher doses, no apparent effect of AKT inhibition and differential selectivity of vinblastine (***Figure 4A***). Next we performed siRNA knockdown of PLK1 and showed inhibition of cell growth in all RDEB SCC populations tested (***Figure 4B***). Four of the populations showed only moderate growth inhibition after PLK1 siRNA (45-75%) and in these cells we performed siRNA knockdown in the presence of vinblastine but failed to see any overt synergy

(***Figure 4C***) as has previously been reported in rhabdomyosarcoma (17). Treatment of RDEB SCC keratinocytes with rigosertib inhibited phosphorylation of both AKT and CRAF which was also evident after PLK1 siRNA knockdown (***Figure S2***).

ON-01910 effectively targets RDEB SCC keratinocytes in vivo

Finally we sought to establish the ability of rigosertib to target RDEB SCC keratinocytes in vivo. Tumor xenograft models showed that either local tumor injection (***Figure S3***) or systemic delivery (***Figure 4***) effectively inhibited the growth of two separate RDEB SCC keratinocyte cell lines in vivo. Ki-67 and TUNEL immuno-histochemistry showed that tumors harvested from those animals treated with rigosertib had significantly fewer proliferative tumor cells and significantly more apoptosis than vehicle control treated animals (***Figure 4D*** and ***E***). Unlike our experiments with BI-2536 (Figure S3 and (10)) we did not see any erythema or ulceration of tissue associated with the injection site when using rigosertib.

Discussion

SCC is a lethal complication for the majority of patients with the already devastating genetic disease RDEB and currently there are no approved or effective therapies for SCC in this patient population (3). Here we present evidence that the multi-kinase inhibitor rigosertib effectively induces apoptosis in 10/10 separate RDEB SCC populations and targets in vivo tumor growth in xenograft studies, data which support a clinical trial of rigosertib in RDEB SCC. In particular, the lack of significant targeting of non-tumor cells by rigosertib (***Figure 2***), the lack of any observed toxicity in our animal studies coupled with the overall favorable side-effect profile for this drug as determined by trials in patients with myelodysplastic syndrome (18) supports the notion that even in a patient group such as RDEB, where numerous clinical complications abound as a result of lack of mechanical integrity of the epidermis, rigosertib may be well tolerated.

Previous studies of rigosertib in the context of head and neck SCC (HNSCC) have demonstrated similar efficacy in a sub-set of tumor cell lines/ populations (19). The data presented in our study show remarkable sensitivity of RDEB SCC to rigosertib and suggests that this subtype of SCC may respond to rigosertib treatment more favorably. We have recently increased our current understanding of RDEB SCC through comprehensive genomic characterization of 27 tumors, including 9/10 cell lines described here (8), which shows that other than mutation burden and mechanism, the somatic mutation profile in RDEB SCC is no different to HNSCC or UV induced skin SCC, and that RDEB SCC are most similar to the basal and mesenchymal sub-types of HNSCC at the level of transcriptomics (8). This similarity to sub-types of HNSCC at the level of mRNA expression may begin to offer opportunity for identifying biomarkers of drug sensitivity and we

are actively pursuing this line of inquiry. Another feature identified in RDEB SCC is homogeneity at the level of somatic tumor driver-gene mutation (8) and this may be advantageous in the context of targeted therapies where resistance that often develops is associated with genetic heterogeneity (20).

With regard to mechanism of action of rigosertib in RDEB SCC we have investigated pathways reported to be targeted by rigosertib and show that only siRNA knockdown of PLK1 has a similar profile in targeting all RDEB SCC cell lines with little effect to normal cells (***Figure 4***). However, the level of PLK1 expression did not seem to show any clear correlation with the sensitivity of individual RDEB SCC cell lines to either PLK1 siRNA or rigosertib, which does not rule out contribution of another pathway when considering RDEB SCC sensitivity to rigosertib over normal cells. Further understanding of this sensitivity may offer precision medicine opportunities for use of rigosertib in subsets of sporadic SCC arising at different anatomical locations and future work will concentrate on understanding the relationship between apoptosis induction and either PLK1 siRNA or rigosertib exposure in RDEB SCC.

Finally, the data described here have supported the approval of a clinical trial comparing the tolerability and efficacy of rigosertib in RDEB SCC (ClinicalTrials.gov Identifier: NCT03786237) and we aim to analyze patient response in the context of biomarker expression, tumor and patient genotype, as well as sensitivity of patient material in the laboratory.

Acknowledgements

This work was supported by DEBRA International – funded by DEBRA UK (grants to APS, and to APS, JB, and JEM) and the Office of the Assistant Secretary of Defense for Health Affairs and the Defense Health Agency J9, Research and Development Directorate, through the Congressionally Directed Medical Research Program under Award No. (W81XWH-18-1-0382 to APS). Opinions, interpretations, conclusions and recommendations are those of the authors and are not necessarily endorsed by the Department of Defense. M.F. is supported by the Sigrid Juse´lius Foundation, Orion Research Foundation, and the Finnish Society of Dermatology. We would like to thank all the patients who contributed to this study, Evan Greenawalt for technical assistance and the Flow Cytometry Shared Resource at the Sidney Kimmel Cancer Center, supported by the NCI, grant 5P30CA056036-17.

References

1. Fine JD, Bruckner-Tuderman L, Eady RA, Bauer EA, Bauer JW, Has C, et al. Inherited epidermolysis bullosa: updated recommendations on diagnosis and classification. J Am Acad Dermatol. 2014;70(6):1103-26.

2. Fine JD, Johnson LB, Weiner M, Li KP, Suchindran C. Epidermolysis bullosa and the risk of life-threatening cancers: the National EB Registry experience, 1986-2006. J Am Acad Dermatol. 2009;60(2):203-11.

3. Mellerio JE, Robertson SJ, Bernardis C, Diem A, Fine JD, George R, et al. Management of cutaneous squamous cell carcinoma in patients with epidermolysis bullosa: best clinical practice guidelines. Br J Dermatol. 2016;174(1):56-67.

4. Christiano AM, Greenspan DS, Hoffman GG, Zhang X, Tamai Y, Lin AN, et al. A missense mutation in type VII collagen in two affected siblings with recessive dystrophic epidermolysis bullosa. Nat Genet. 1993;4(1):62-6.

5. Mellerio JE, Weiner M, Denyer JE, Pillay EI, Lucky AW, Bruckner A, et al. Medical management of epidermolysis bullosa: Proceedings of the IInd International Symposium on Epidermolysis Bullosa, Santiago, Chile, 2005. Int J Dermatol. 2007;46(8):795-800.

6. Ng YZ, Pourreyron C, Salas-Alanis JC, Dayal JH, Cepeda-Valdes R, Yan W, et al. Fibroblast-derived dermal matrix drives development of aggressive cutaneous squamous cell carcinoma in patients with recessive dystrophic epidermolysis bullosa. Cancer Res. 2012;72(14):3522-34.

7. Mittapalli VR, Madl J, Loffek S, Kiritsi D, Kern JS, Romer W, et al. Injury-Driven Stiffening of the Dermis Expedites Skin Carcinoma Progression. Cancer Res. 2016;76(4):940-51.

8. Cho RJ, Alexandrov LB, den Breems NY, Atanasova VS, Farshchian M, Purdom E, et al. APOBEC mutation drives early-onset squamous cell carcinomas in recessive dystrophic epidermolysis bullosa. Sci. Trans. Med. 2018;10:eaas9668. DOI: 10.1126/scitranslmed.aas9668

9. Purdie KJ, Pourreyron C, Fassihi H, Cepeda-Valdes R, Frew JW, Volz A, et al. No evidence that human papillomavirus is responsible for the aggressive nature of recessive dystrophic epidermolysis bullosa-associated squamous cell carcinoma. J Invest Dermatol. 2010;130(12):2853-5.

10. Watt SA, Pourreyron C, Purdie K, Hogan C, Cole CL, Foster N, et al. Integrative mRNA profiling comparing cultured primary cells with clinical samples reveals PLK1 and C20orf20 as therapeutic targets in cutaneous squamous cell carcinoma. Oncogene. 2011;30(46):4666-77.

11. Purdie KJ, Pourreyron C, South AP. Isolation and culture of squamous cell carcinoma lines. Methods Mol Biol. 2011;731:151-9.

12. Chapman CM, Sun X, Roschewski M, Aue G, Farooqui M, Stennett L, et al. ON 01910.Na is selectively cytotoxic for chronic lymphocytic leukemia cells through a dual mechanism of action involving PI3K/AKT inhibition and induction of oxidative stress. Clin Cancer Res. 2012;18(7):1979-91.

13. Prasad A, Khudaynazar N, Tantravahi RV, Gillum AM, Hoffman BS. ON 01910.Na (rigosertib) inhibits PI3K/Akt pathway and activates oxidative stress signals in head and neck cancer cell lines. Oncotarget. 2016.

14. Prasad A, Park IW, Allen H, Zhang X, Reddy MV, Boominathan R, et al. Styryl sulfonyl compounds inhibit translation of cyclin D1 in mantle cell lymphoma cells. Oncogene. 2009;28(12):1518-28.

15. Athuluri-Divakar SK, Vasquez-Del Carpio R, Dutta K, Baker SJ, Cosenza SC, Basu I, et al. A Small Molecule RAS-Mimetic Disrupts RAS Association with Effector Proteins to Block Signaling. Cell. 2016;165(3):643-55.

16. Jost M, Chen Y, Gilbert LA, Horlbeck MA, Krenning L, Menchon G, et al. Combined CRISPRi/a-Based Chemical Genetic Screens Reveal that Rigosertib Is a Microtubule-Destabilizing Agent. Mol Cell. 2017; 68(1):210-223.

17. Hugle M, Belz K, Fulda S. Identification of synthetic lethality of PLK1 inhibition and microtubule-destabilizing drugs. Cell Death Differ. 2015; 22(12):1946-56.

18. Silverman LR, Greenberg P, Raza A, Olnes MJ, Holland JF, Reddy P, et al. Clinical activity and safety of the dual pathway inhibitor rigosertib for higher risk myelodysplastic syndromes following DNA methyltransferase inhibitor therapy. Hematol Oncol. 2015;33(2):57-66.

19. Anderson RT, Keysar SB, Bowles DW, Glogowska MJ, Astling DP, Morton JJ, et al. The dual pathway inhibitor rigosertib is effective in direct patient tumor xenografts of head and neck squamous cell carcinomas. Mol Cancer Ther. 2013;12(10):1994-2005.

20. Konieczkowski DJ1, Johannessen CM2, Garraway LA. A Convergence-Based Framework for Cancer Drug Resistance. Cancer Cell. 2018 33(5):801-815.

Tables

Table 1:

EC_{50} (μM) values as determined by crystal violet assay for 10 RDEB SCC cell lines.

Cell Line	μM
SCCRDEB2	0.1731
SCCRDEB3	0.2198
SCCRDEB4	0.1647
SCCRDEB53	1.567
SCCRDEB62	0.1977
SCCRDEB70	0.1741
SCCRDEB71	0.2165
SCCRDEB99	0.2197
SCCRDEB106	0.1496
SCCRDEB108	0.0834

Figure Legends

Figure 1: *PLK1 is increased in RDEB SCC*

A: 5μg of total cell lysate was resolved on a 6% SDS PAGE gel, transferred to nitrocellulose membrane before being incubated with antibodies raised against PLK1 (Cell Signaling, 208G4) and GAPDH (Santa Cruz Biotechnology, 6C5). Samples loaded from left to right: lanes 1-2 = normal primary breast keratinocytes (Br61, Br63), lanes 3-6 = RDEB primary keratinocytes (RDEB81, RDEB84, RDEB85, and RDEB118), lanes 7-14 = RDEB SCC keratinocytes (SCCRDEB108, SCCRDEB2, SCCRDEB3, SCCRDEB70, SCCRDEB71, SCCRDEB4, SCCRDEB62, and SCCRDEB106). **B**: 6μM frozen sections were processed and incubated with an antibody raised against PLK1 (Sigma-Aldrich, HPA053229) (red) as well as the nuclear stain DAPI (blue). Bar = 400μM.

Figure 2: *Rigosertib effectively targets RDEB SCC keratinocytes in vitro*

A: Normal primary keratinocytes (FS1, Br61), RDEB primary keratinocytes (RDEB81, RDEB84), and RDEB SCC keratinocytes (SCCRDEB2, SCCRDEB3, SCCRDEB4) were seeded into wells of a 96 well plate and exposed to vehicle (DMSO) or increasing concentrations of rigosertib (0.01-100uM) for 48 hrs. Cells were then fixed with 70% ETOH and incubated with the cell dye crystal violet. Plate was photographed after excess dye was washed away with water. **B**: Crystal violet retention was measured using a spectrometer and values relative to vehicle alone were calculated for cells exposed to increasing concentrations of rigosertib. Left graph shows response curve (±SD) from a single experiment using 4 populations of primary non-SCC keratinocytes (Br61, Br63, RDEB81, RDEB84) and 10 populations of RDEB SCC keratinocytes. Right graph shows results for RDEB SCC

cells shown in **A** after exposure to a wider range of drug concentrations used to determine EC_{50} values for all 10 populations of RDEB SCCC keratinocytes (see ***Table 1*** *and* ***Figure S1***). **C**: Cells were plated into a 6-well plate and incubated with vehicle alone or 1uM of rigosertib for 48 hrs before photographs were taken. Br63 (Primary normal) and SCCRDEB3 cells are shown.

Figure 3: *Rigosertib induces G2M arrest and apoptosis in RDEB SCC keratinocytes*

A: Cell-cycle analysis in either RDEB SCC keratinocytes (SCCRDEB2, SCCRDEB3, SCCRDEB4, SCCRDEB53, and SCCRDEB106) or non-SCC keratinocytes (Br61, RDEB115, RDEB124) treated with rigosertib (1uM, Non-SCC treated and SCC treated) or vehicle control (Non-SCC untreated and SCC untreated), and stained for BrdU and propidium iodide. Results expressed as percentage of cells at the G0/G1, S and G2/M phases of cell cycle 16 h following treatment. The results shown are the mean (±SD) **B**: Graph shows relative mean absorbance increase using a colorimetric assay to detect cleaved nucleosomes in the cytoplasm as a measure of apoptosis after exposure of cells to vehicle or rigosertib. Data shown are the mean (±SD) from two independent experiments using 2 populations of normal primary keratinocytes (Br46, Br61), 3 populations of primary RDEB keratinocytes (RDEB81, RDEB84, RDEB86) and 10 populations of RDEB SCC keratinocytes (***Table S1***) exposed to 1μM of rigosertib for 16-24 hrs. * = $p < 0.05$, ** = $p < 0.005$ (Student t-test).

Figure 4: *Rigosertib specificity mirrors PLK1 siRNA knockdown in RDEB SCC keratinocytes*

RDEB SCC keratinocytes (n=9) were exposed to AKT and MEK inhibitors, the microtubule disrupting agent vinblastine and PLK1 siRNA knockdown. **A**: Cells were seeded into wells of a 96 well plate and exposed to vehicle (DMSO) or drug for 48 hrs. Cells were then fixed with 70% ETOH

and crystal violet retention was measured using a spectrometer and values relative to vehicle alone (100%) were plotted. For each cell line bars indicate the following, left to right: A = AKT inhibitor LY294002 0.1μM and 5μM, T = trametinib 0.1μM and 1μM, C = cobimetinib 2μM and 5μM, V = vinblastine 0.1μM and 5μM. **B**: Cells were seeded into wells of duplicate 6 well plates and transfected with PLK1 siRNA, scrambled control or a cell death control siRNA. 16 hours later one set of cells were trypsinized and transferred to 96 well plates before being fixed 48 hrs later. Total cell lysates were isolated from duplicate 6 well plates at the same time as the 96 well re-seeded plates were fixed. Graph shows cell growth relative to scrambled control siRNA after staining with crystal violet while images below show immuno-blotting results with antibodies raised against PLK1 (Cell Signaling, 208G4) and GAPDH (Santa Cruz Biotechnology, 6C5). **+** = PLK1 siRNA, **-** = scrambled control siRNA. **C**: Cells were seeded directly into wells of a 96 well plate and transfected with PLK1 siRNA, scrambled control or a cell death control siRNA. 16 hours later cells were treated with 1μM vinblastine before being fixed 48 hrs later. Graph shows cell growth relative to scrambled control siRNA after staining with crystal violet.

Figure 5: *Rigosertib effectively targets RDEB SCC keratinocytes in vivo*

Animals bearing SCCRDEB106 xenograft tumors that had reached >100mm^3 were treated with either rigosertib (n=4) or vehicle control (n=4) injected IP every day for 14 days. Tumors were measured with calipers (**A**) until day 15 when animals were sacrificed, tumors were harvested, weighed (**B**) and photographed (**C**) before being bisected and frozen or fixed with formalin and paraffin embedded. **D**: 4uM FFPE sections were cut and incubated with an antibody recognizing

Ki-67 (Abcam, ab16667, 1:200) as well as the nuclear stain hematoxylin. Graph shows the number of Ki-67 positive nuclei manually counted from five distinct microscopic fields for each tumor (n=8) at 20× magnification. **E**: 4μM FFPE sections were cut and incubated with an antibody recognizing TUNEL (HERE) as well as the nuclear stain DAPI. Graph shows the number of TUNEL positive nuclei per cell calculated using ImageJ software. * = $p < 0.05$, ** = $p < 0.01$, *** = $p < 0.001$ (Student t-test).

Figure 1

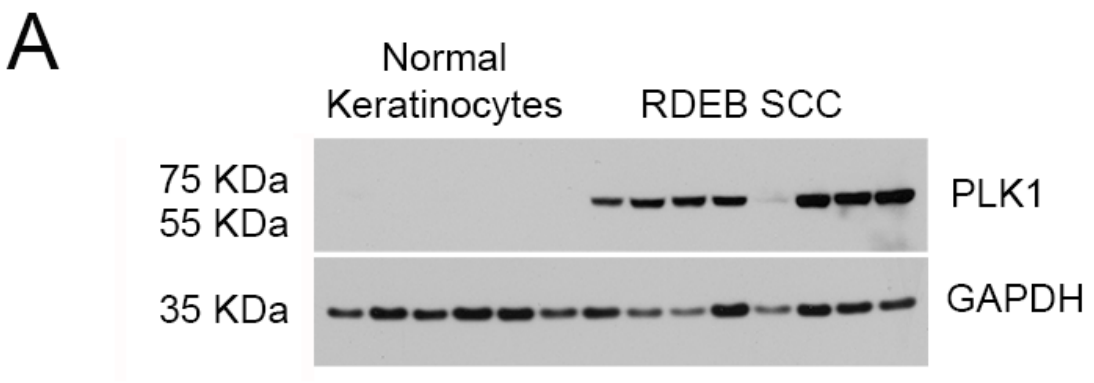

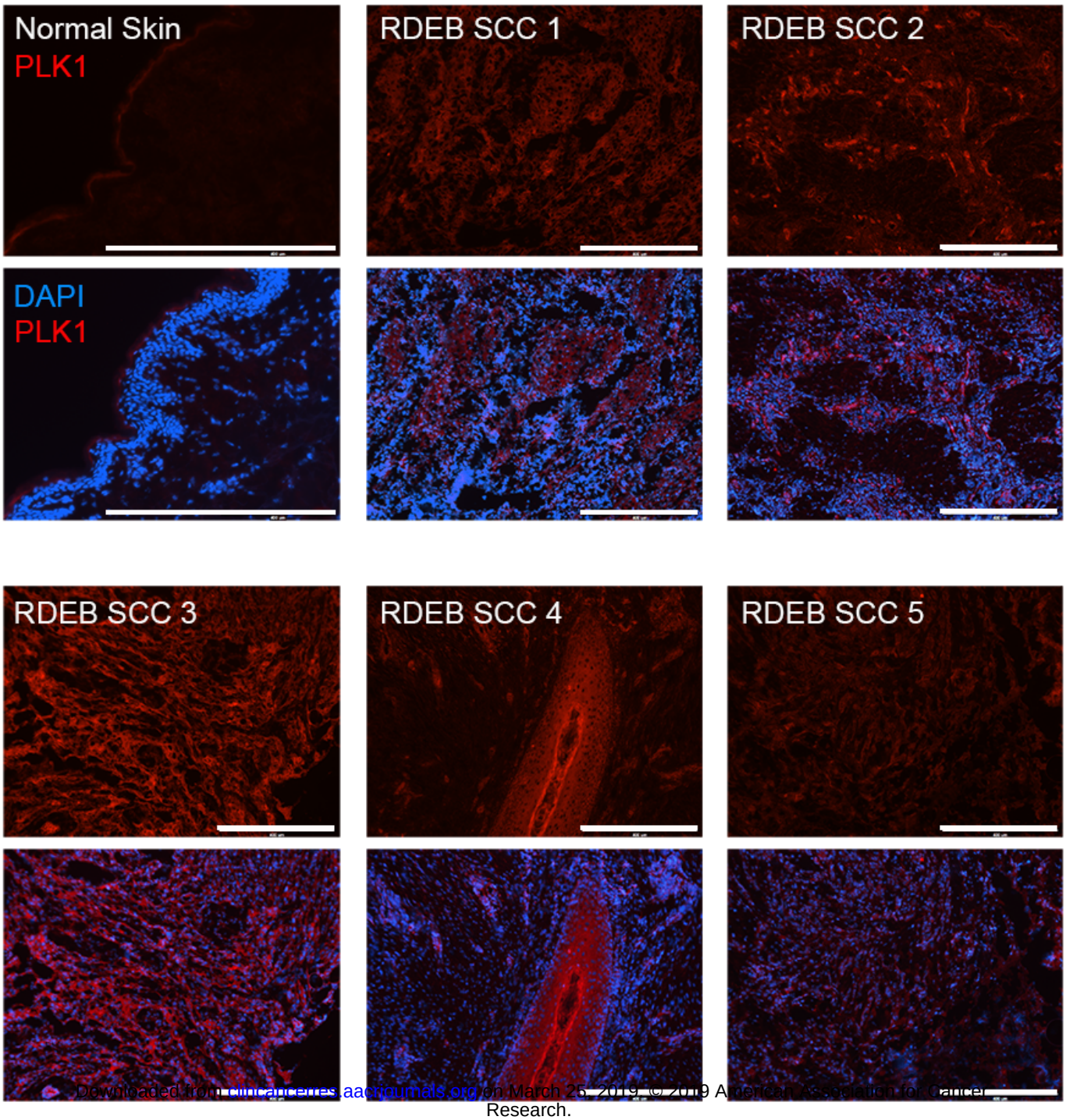

Figure 2

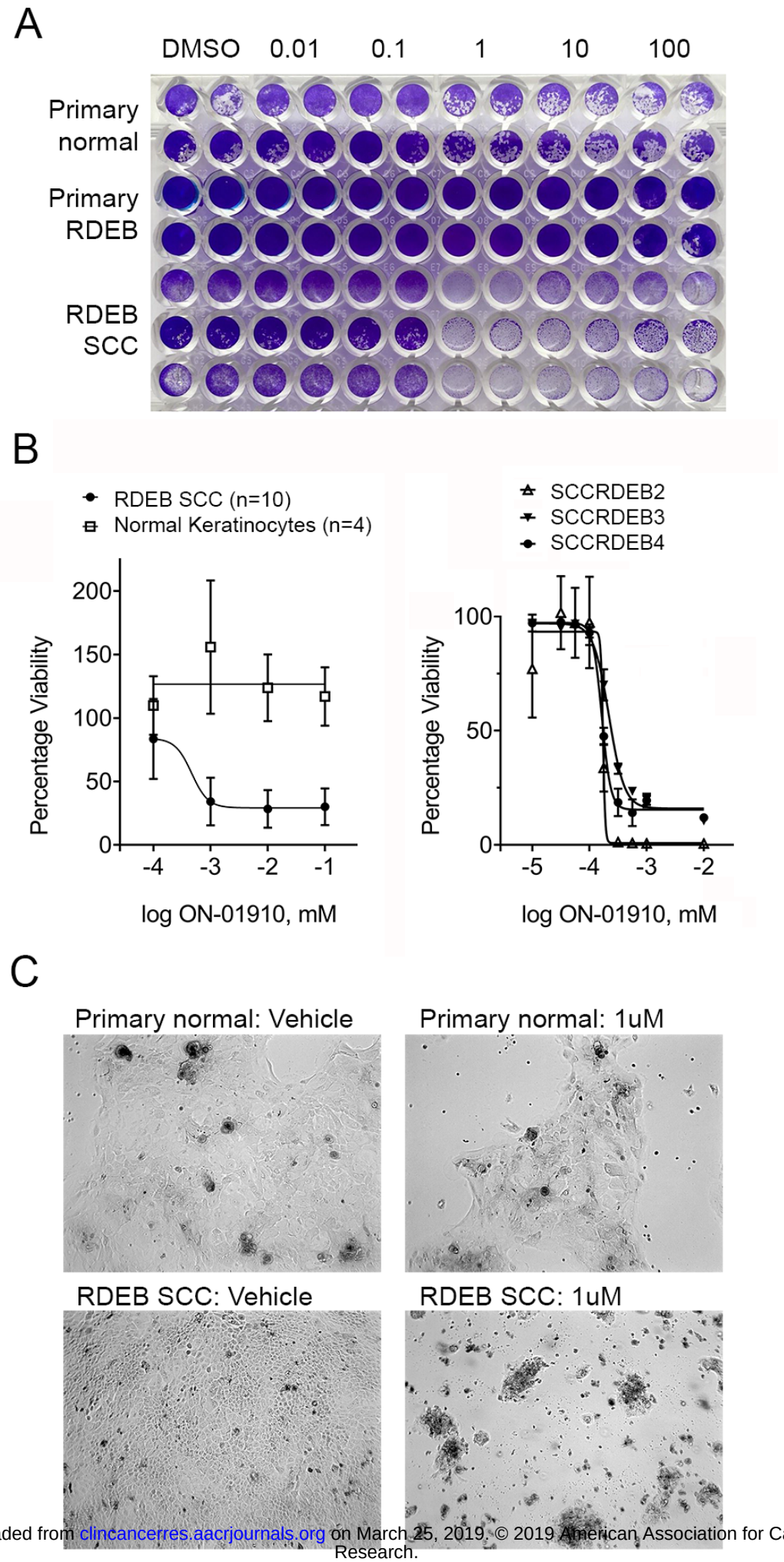

Figure 3

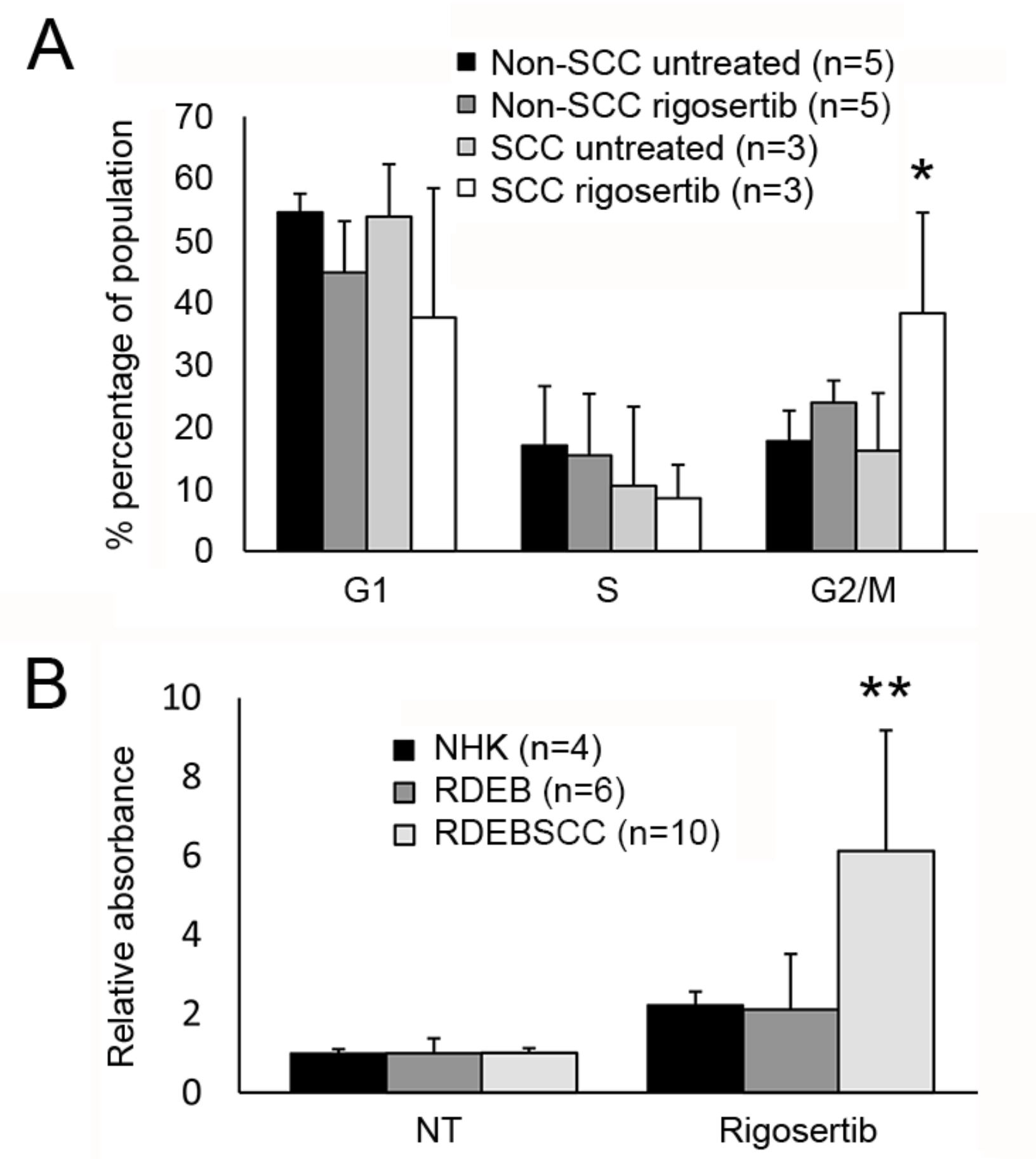

Figure 4

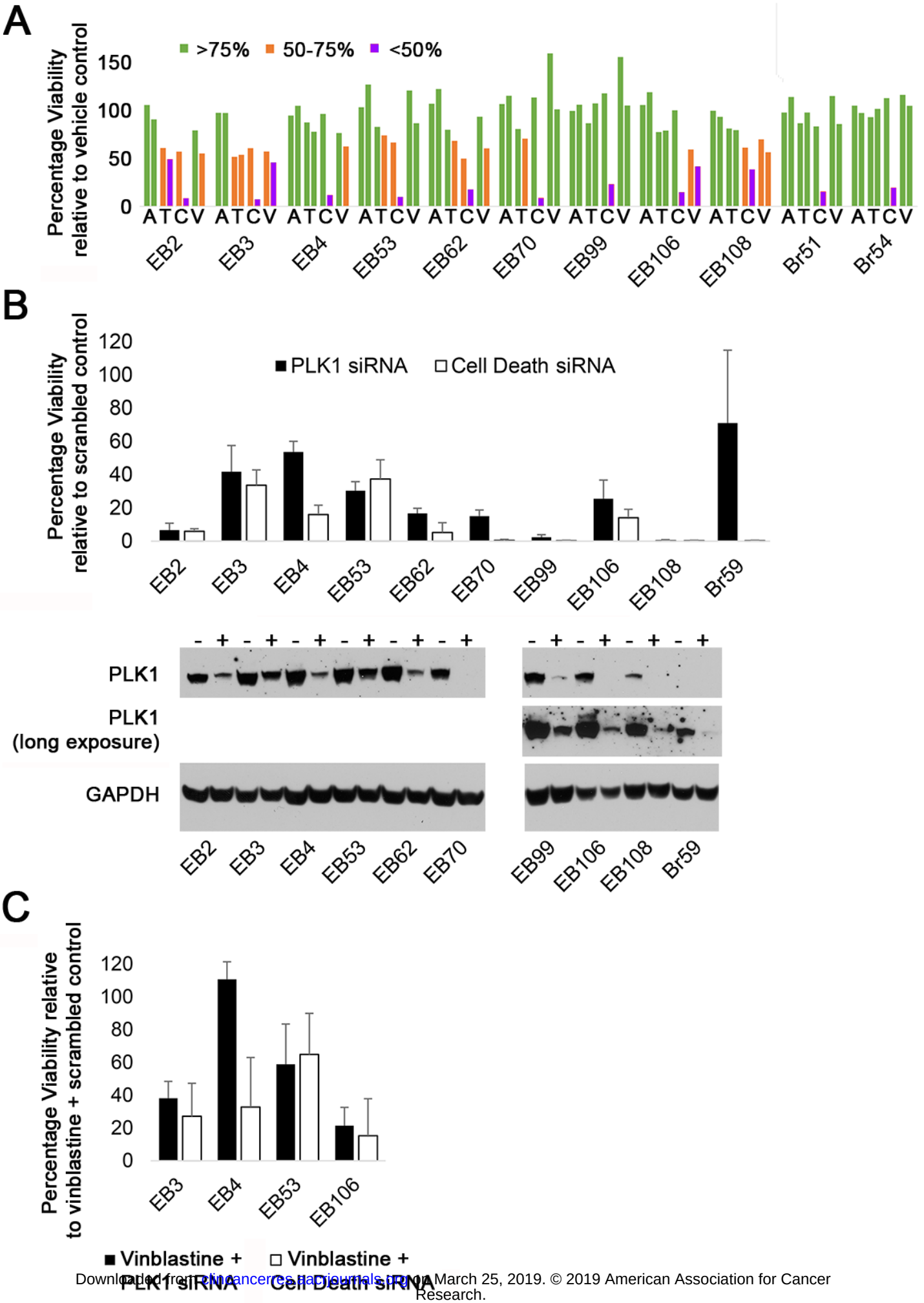

Author Manuscript Published OnlineFirst on March 7, 2019; DOI: 10.1158/1078-0432.CCR-18-2661
Author manuscripts have been peer reviewed and accepted for publication but have not yet been edited.

Figure 5

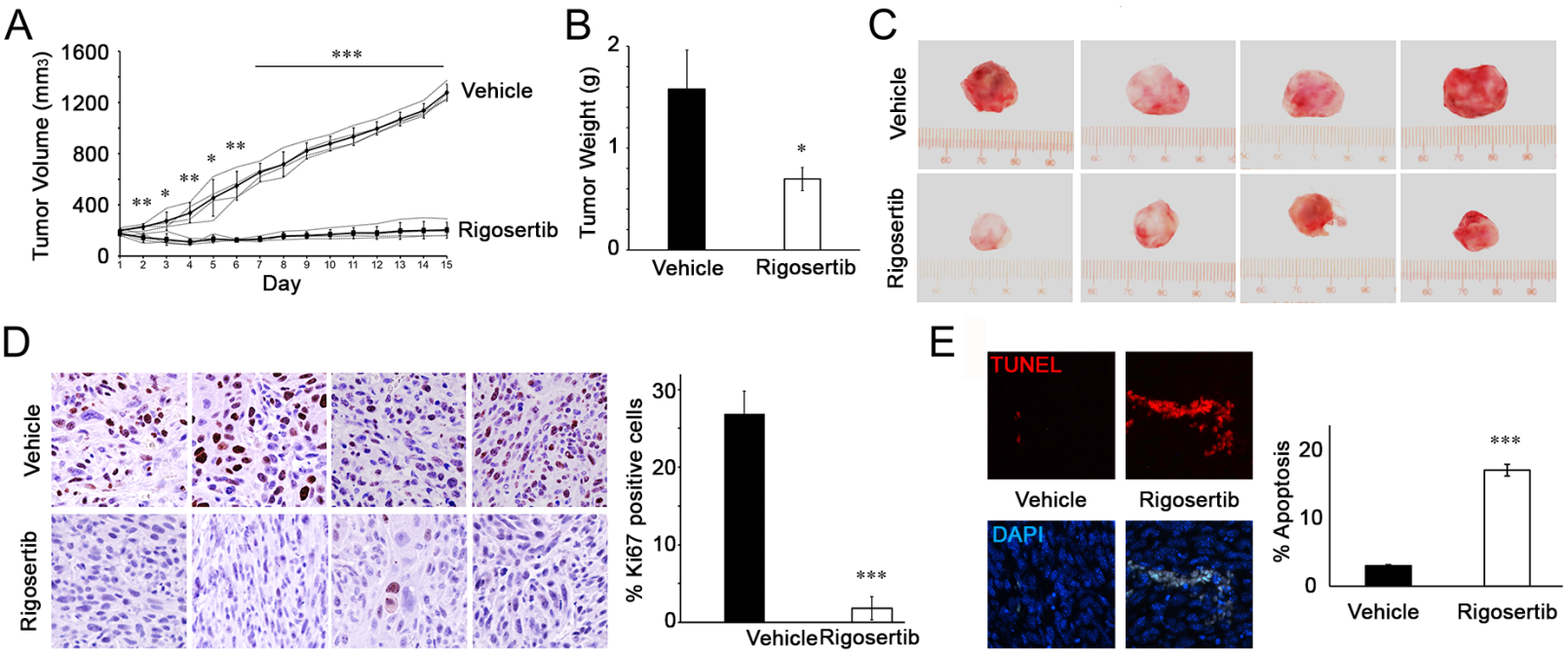

AACR American Association for Cancer Research

Clinical Cancer Research

Identification of rigosertib for the treatment of recessive dystrophic epidermolysis bullosa-associated squamous cell carcinoma

Velina S. Atanasova, Celine Pourreyron, Mehdi Farshchian, et al.

Clin Cancer Res Published OnlineFirst March 7, 2019.